Earthquakes and Structures, *Vol. 15, No. 3 (2018) 335-350*
DOI: https://doi.org/10.12989/eas.2018.15.3.335

Ambient vibration based structural evaluation of reinforced concrete building model

Murat Gunaydin*, Suleyman Adanur and Ahmet C. Altunisik

Department of Civil Engineering, Karadeniz Technical University, Trabzon, Turkey

(Received November 2, 2017, Revised August 2, 2018, Accepted August 3, 2018)

Abstract. This paper presents numerical modelling, modal testing, finite element model updating, linear and nonlinear earthquake behavior of a reinforced concrete building model. A 1/2 geometrically scale, two-storey, reinforced concrete frame model with raft base were constructed, tested and analyzed. Modal testing on the model using ambient vibrations is performed to illustrate the dynamic characteristics experimentally. Finite element model of the structure is developed by ANSYS software and dynamic characteristics such as natural frequencies, mode shapes and damping ratios are calculated numerically. The enhanced frequency domain decomposition method and the stochastic subspace identification method are used for identifying dynamic characteristics experimentally and such values are used to update the finite element models. Different parameters of the model are calibrated using manual tuning process to minimize the differences between the numerically calculated and experimentally measured dynamic characteristics. The maximum difference between the measured and numerically calculated frequencies is reduced from 28.47% to 4.75% with the model updating. To determine the effects of the finite element model updating on the earthquake behavior, linear and nonlinear earthquake analyses are performed using 1992 Erzincan earthquake record, before and after model updating. After model updating, the maximum differences in the displacements and stresses were obtained as 29% and 25% for the linear earthquake analysis and 28% and 47% for the nonlinear earthquake analysis compared with that obtained from initial earthquake results before model updating. These differences state that finite element model updating provides a significant influence on linear and especially nonlinear earthquake behavior of buildings.

Keywords: ambient vibration testing; dynamics characteristics; linear earthquake behavior; nonlinear earthquake behavior; finite element model updating

1. Introduction

In structural engineering, much effort is devoted to obtain accurate finite element models of structures. These models are used in many civil engineering applications such as damage detection, linear and nonlinear dynamic behavior under different loads, structural health monitoring, remaining lifetime of special structures, structural elevation i.e., retrofitting (Jaishi and Ren 2005, Ribeiro *et al*. 2012). However, depending on some uncertain parameters such as material properties, boundary conditions and mesh sizes considered in the finite element models, the accurate finite element models cannot be achieved with the required level of accuracy. The low accuracy models can cause erroneous results and may be detrimental in the calculation of the dynamic characteristics which are the key parameters in determining the structural behavior especially in earthquake response. Therefore, the finite element model must be updated by experimental measurements to obtain more accurate models and results.

Modal testing using vibration measurements have been commonly used to update the finite element (FE) models. Updating of a FE model with experimental measurements, also called as FE model updating, is a process to modify the uncertain parameters in the finite element models. The main purpose of this is to minimize the differences between the numerical and experimental dynamic characteristics, namely natural frequency and mode shapes.

Modal testing is a popular method used to extract data on dynamic characteristics of structures. Two methods, called as Experimental Modal Analysis (EMA) and Operational Modal Analysis (OMA) have currently been used to obtain the dynamic characteristics of structures experimentally. In EMA, the structures vibrate by a known input force using artificially excited such as impulse hammer, hydraulic shaker, and response of structures measure. In OMA, the structures vibrate by an unknown input force using natural excitations such as earthquake, wind, blasting and response of structures measure. Hence, this method is also called as Ambient Vibration Testing (AVT). It should be noted that, excitation of structures in operational condition is not cheap and easy. So, AVT are quite attractive according to EMA because of being inexpensive since extra equipment is not needed to vibrate the structures.

Many studies of modal testing have been carried out by different researchers. Modal testing can be used in various ways such as structural damage detection, finite element model updating, structural safety evaluation, structural health monitoring, estimating dynamic behavior, and

*Corresponding author, Assistant Professor
E-mail: muratgunaydin@ktu.edu.tr
mgunaydin@gumushane.edu.tr

Copyright © 2018 Techno-Press, Ltd.
http://www.techno-press.com/journals/eas&subpage=7
ISSN: 2092-7614 (Print), 2092-7622 (Online)

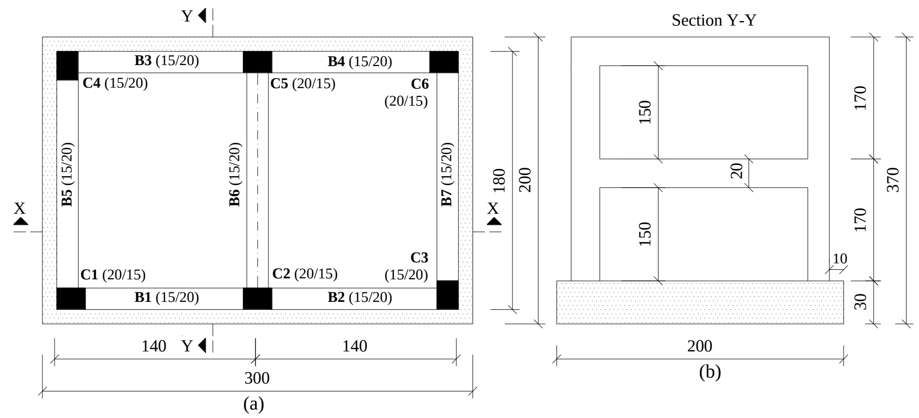

Fig. 1 Floor plan view (a) and its lateral view (b) of frame

estimating the effectiveness of repairing or strengthening techniques (Friswell and Mottershead 1995, Hassiotis and Jeong 1995, Doebling *et al.* 1996, Alampalli 2000, Peeters 2000, Ren and De Roeck 2002a, b, Kaiser and Karbhari 2004, Bonfiglioli and Pascale 2006). Modal testing has been successfully used by researchers for the different types of structures and/or scale structures such as dams (Deinum *et al.* 1982, Loh and Wu 1996, Ziyad 1998, Proulx *et al.* 2001, Oliveria and Mendes 2006, Wang and He 2007, Sevim *et al*. 2011, Altunışık *et al*. 2015, Yang *et al*. 2017), bridges (Brownjohn *et al*. 1992, Brownjohn 1997, Chang *et al*. 2001, Ren *et al*. 2004, Jaishi *et al*. 2007, Altunışık *et al*. 2011, Ribeiro *et al*. 2012, Cantero *et al*. 2017, Chen *et al*. 2017), buildings and towers (Venturaet *et al*. 2002, Wu and Li 2004, Sortis *et al*. 2005, Skolnik *et al*. (2007), Zhou *et al*. 2007, Zonta *et al*. 2008, Türker and Bayraktar 2014, S. Kouris *et al*. 2017, Park *et al*. 2018, Diaferio *et al*. 2018).

To the best of the authors' knowledge, investigations into modal testing, finite element model updating and in particular the effects of model updating on the both linear and nonlinear earthquake behavior of buildings are rare. The contribution of the current study may assist in alleviating this situation. To this end, a 1/2 geometrically scale, two-storey, reinforced concrete frame model is considered as sample for examining the effects of the model updating on the linear and nonlinear earthquake behavior.

2. Scaled frame model

2.1 Model design and construction phase

The reinforced concrete (RC) model tested in this study was a geometrically scaled frame constructed in the laboratory. The frame was 180 cm×280 cm in plan and had a constant storey height of 170 cm. The model had two bays in the longitudinal direction and one bay in the transverse direction. The model was built on a rigid foundation of 200×300×30 cm (width×length×height). The cross-section of beams was 15 cm×20 cm, whilst four columns had rectangular cross-sections of 20×15 cm and two columns had a rectangular cross-section of 15×20 cm. The model floor plan and its lateral view are shown in Fig. 1.

Four ten-millimeter deformed bars were used as column longitudinal reinforcement. The longitudinal bars were continued from the bottom of the foundation to the top of the columns. Two ten-millimeter deformed bars at the top and bottom were used for the longitudinal reinforcement of the beams. The columns and beams were reinforced using transverse stirrups of eight-millimeter diameter spaced at 25 cm. The thickness of rigid foundation was 30 cm. The foundation was reinforced with a bi-directional grid of ten-millimeter deformed bars, spaced at 20 cm in the transverse and longitudinal directions. Clear covers were considered as 2.5 cm for the beams, columns and foundations. A general view of the frame along with details of the general geometry, element sections and corresponding reinforced layout are shown in Fig. 2.

The RC frame model was poured vertically by wooden formwork with design compressive strengths of 16 and 12 MPa for rigid foundation and frame, respectively. The ready-mixed concrete was used. The foundation construction began in September 2014 (Fig. 3). The first story construction of the frame started in October 2014. Fifty five days after casting, the second story construction was begun. The vibrator was used at each stage of casting. The wooden formworks were removed three weeks later after casting. Fig. 4 shows some construction stages for the RC frame model.

3. Experimental dynamic characteristics

The experimental dynamic characteristics were obtained using AVT. With the aim of the identifying dynamic characteristics such as natural frequencies, mode shapes and damping ratios, the AVT was implemented on the model. Many dynamic characteristics identification methods have used for extracting the dynamic characteristics. These are the Operating Vectors Method, the Complex Exponential Method, the Polyreference Time Domain Method, the Enhanced Frequency Domain Decomposition (EFDD) and Stochastic Subspace Identification (SSI) methods. In the study, EFDD in the frequency domain and SSI in the time domain were used. Detail information about the both methods can be found in the literature (Ewins 1984, Felber 1993, Peeters 2000, Bendat *et al*. 2004, Jacabsen *et al.* 2006, Rainieri *et al*. 2007).

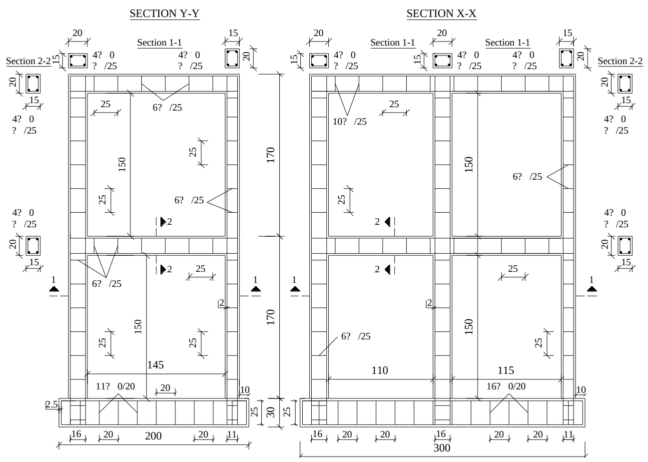

Fig. 2 Dimensions and reinforcement layouts of the model (dimension in cm)

Fig. 3 Foundation construction

(a) Formwork assembly for columns and beams

(b) Placement of the reinforcements

(c) Casting of the RC model

Fig. 4 Construction stages for the RC model

After 45 and 60 days from the first and second story construction, the AVT measurements were separately implemented on the single-story and two-story model.

During the AVT measurement a B&K 3560 data acquisition system with 17 channels and B&K 8340-type

Fig. 5 The accelerometers connection with steel dowels

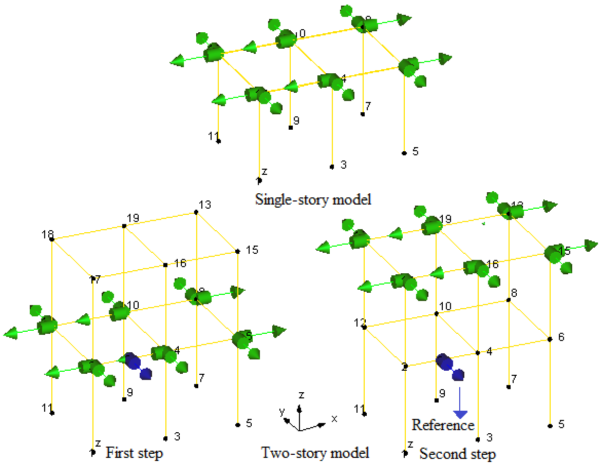

Fig. 6 Accelerometers layout considered in the AVTs

uni-axial accelerometers, a notebook, PULSE and Operational Modal Analysis software were used. The accelerometers had 10 V/g sensitivity. For measurements, the frequency ranges were selected as 0-100 Hz and 0-50 Hz for the first and second story model, respectively. The B&K 3560 acquired the data and transferred them to PULSE Labshop software (PULSE 2006). Operational Modal Analysis software (OMA 2006) was used to estimate the dynamic properties. These accelerometers were attached to the beam-column joints using steel dowels in transverse and longitudinal directions (Fig. 5).

In the measurements, thirteen accelerometers were employed and were carried out during ten-minute intervals. Due to the limited number of accelerometers and channels in data acquisition system, one of the accelerometers was used as a reference accelerometer. Twelve accelerometers were moved from one story to another and obtained signals from each story were combined by the reference accelerometer. Hence, the measurements of two-story model were performed in two separate steps. Fig. 6 presents the location of the accelerometers on the single-story and two-story model.

3.2 Ambient vibration test for the single story model

The AVT measurement was firstly carried out on the single-story model. The dynamic characteristics of single-story model were attained with EFDD and SSI methods. The singular values of spectral density matrices (SVSDM) and stabilization diagram of estimated state-space models obtained from vibration signals by the EFDD and SSI methods for the single-story model are shown in Fig. 7. As seen in Fig. 7, natural frequencies were obtained within the

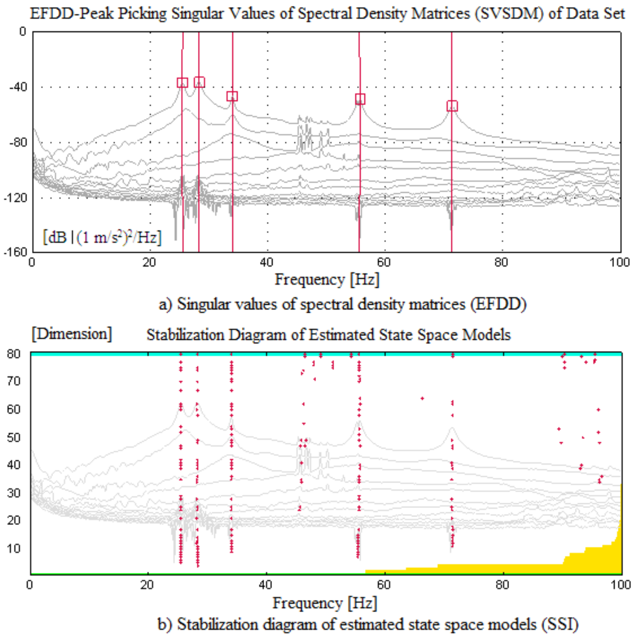

Fig. 7 Dynamic characteristics of the single-story model for (a) EFDD and (b) SSI

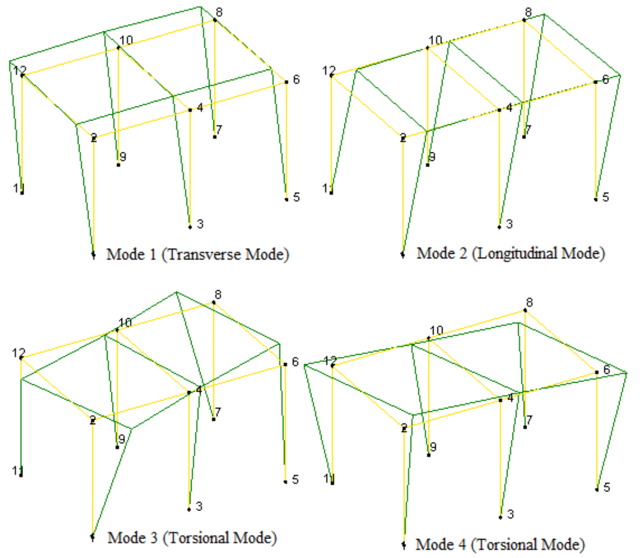

Fig. 8 The first four mode shapes for the single-story model

0-100 Hz frequency range.

The first four mode shapes for the single-story model are shown in Fig. 8. As seen in Fig. 8, the first one is transverse mode, the second one is longitudinal mode, and the third and fourth are torsional mode.

The modal assurance criterion (MAC) graphics are widely plotted to evaluate the correlation of mode shapes. The graphic are automatically calculated by OMA software. Fig. 9 shows the MAC graphics estimated using EFDD and SSI methods for the single-story model. Fig. 9 shows that the correlation of the mode shapes reflected by MAC values seems so good. For each modes, the MAC values are high (between 0.95-0.99) It is mean that EFDD and SSI results are almost the same. The natural frequencies and damping ratios identified with EFDD and SSI methods for the single-story model are given in Table 1. Table 1 show that the natural frequencies correlations for the EFDD and SSI methods are so close. But there is no clear agreement between damping ratios.

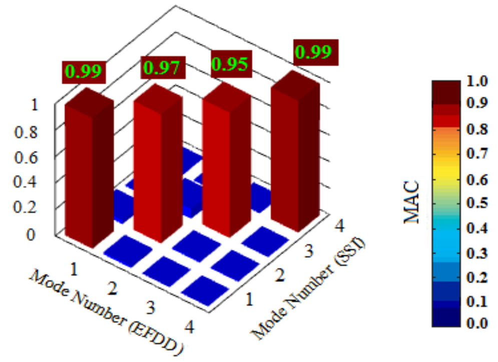

Fig. 9 MAC graphic estimated by EFDD and SSI methods for the single-story model

Table 1 Natural frequencies obtained from single story model for the EFDD and SSI

Node	Frequency (Hz)		Damping Ratio (%)	
	EFDD	SSI	EFDD	SSI
1	25.54	25.53	1.3200	0.6018
2	28.30	28.27	1.5910	1.3790
3	34.03	33.98	0.5684	0.4071
4	55.61	55.55	0.8043	0.7499

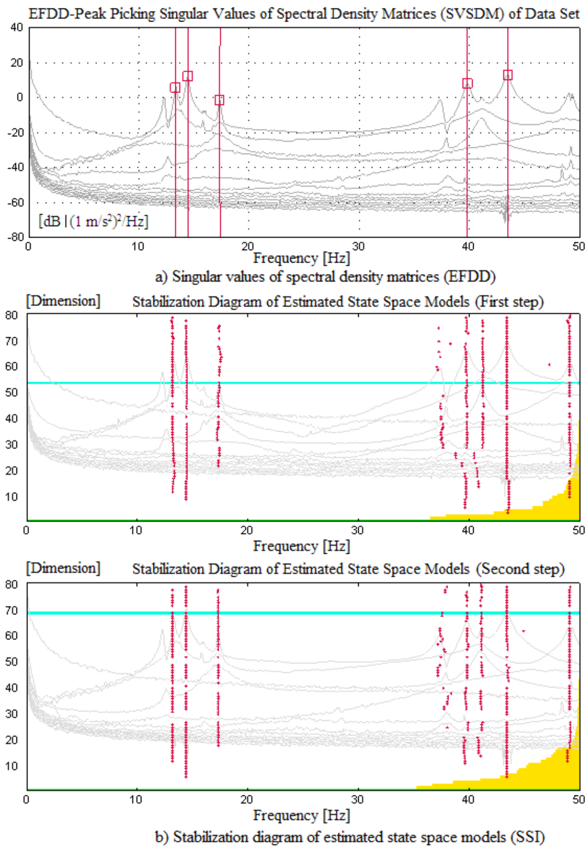

Fig. 10 Dynamic characteristics of the two-story model attained for EFDD and SSI

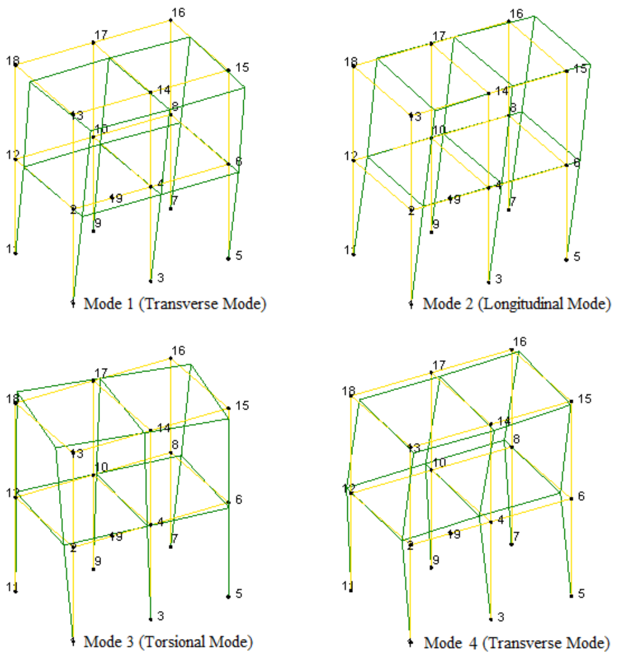

Fig. 11 The first four mode shapes for the two-story model

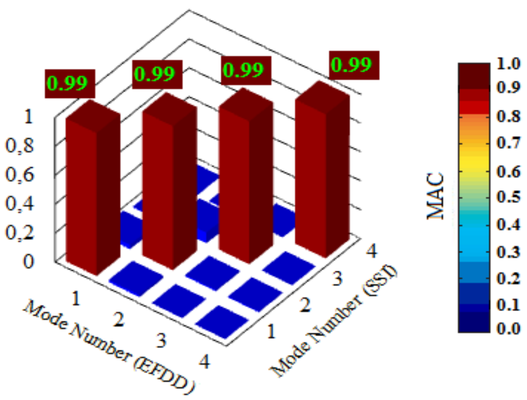

Fig. 12 MAC graphic estimated by EFDD and SSI methods for the two-story model

3.3 Ambient vibration test for the two-story model

After 60 days from the construction of two-story model, AVT measurement was performed on the two-story model. SVSDM and stabilization diagram of estimated state-space models obtained from vibration signals by the EFDD and SSI methods for the two-story model are shown in Fig. 10. The first five natural frequencies obtained were within the 0-50 Hz frequency range. Fig. 11 illustrates first four mode shapes obtained from the AVT measurement for the two-story model. The first one is transverse mode, the second one is longitudinal mode, the third one is torsional mode and fourth is transverse mode.

The modal assurance criterion (MAC) graphics are also plotted (Fig. 12) for the two-story model to evaluate the correlation of mode shapes obtained between the EFDD and SSI methods. Fig. 12 clearly shows the pairing of mode shapes obtained between the EFDD and SSI methods seems good. The natural frequencies and damping ratios expressed by the EFDD and SSI methods for the two-story model are given in Table 2. The first four natural frequencies were obtained within 13.36 Hz-39.82 Hz, and 13.20 Hz-39.81 Hz for the EFDD and SSI methods, respectively. Table 2 shows that the natural frequencies correlations for the EFDD and SSI methods are good. But, there is no clear agreement between damping ratios.

Table 2 Natural frequencies obtained from two-story model for the EFDD and SSI

Node	Frequency (Hz)		Damping Ratio (%)	
	EFDD	SSI	EFDD	SSI
1	13.36	13.20	0.7119	1.2580
2	14.45	14.44	0.7267	0.7080
3	17.38	17.36	0.4717	0.7204
4	39.82	39.81	0.6386	0.4895

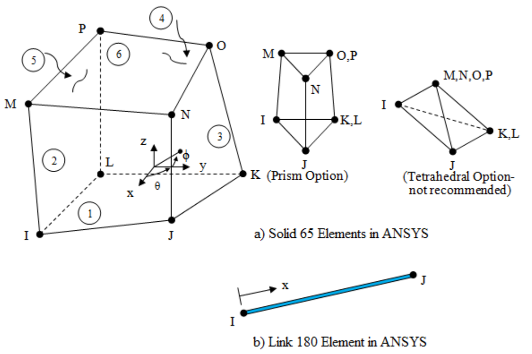

Fig. 13 SOLID65 and LINK180 elements in ANSYS

4. Finite element model and model updating

This section presents the finite element (FE) models and model updating of single and two story models. Initial finite FE models were developed using ANSYS (2015) software to obtain the dynamic characteristics such as frequencies and mode shapes. The term of "initial" has generally used to represent the inaccurate FE model which is the basis for the model updating procedure. Model development and updating was carried out two distinct phases. The first phase was the creation of the initial FE model for the single and two story models. The second phase was the updating procedure of the single-story and two-story model according to the AVT measurement results.

4.1 Initial FE models for single-story and two-story models

The initial FE models created in ANSYS have the same geometry and reinforcement layout with the constructed models. The SOLID65 element type was used to identify the properties of concrete in the FE models. This element is suitable for the three dimensional modeling of concrete with or without reinforcing rebar. In addition, it is capable of cracking in tension and crushing in compression. The element is also capable of plastic deformation and creep. The element has eight nodes, and each node has three degrees of freedom namely translations in the nodal *x*, *y* and *z* directions. In addition, LINK180 element having two nodes was used to simulate discrete steel reinforcement (ANSYS 2015). The geometry and node locations for these elements are shown in Fig. 13.

The SOLID65 and LINK180 elements require input data for materials such as modulus of elasticity, Poisson's ratio and unit weight. The design compressive strengths are 16 MPA and 12 MPa for the rigid foundation and frame, respectively. These were taken into account in the calculation of elasticity modulus for the initial FE model using Eq. (1) (ACI 318M-2008).

$$E = 0.043 \times w_c^{1.5} \sqrt{f_c^{'}} \tag{1}$$

In Eq. (1), E is the modulus of elasticity, $w_c^{1.5}$ is the unit weight of the concrete, $f_c^{'}$ is the characteristic cylinder strength at 28 days (MPa), respectively. The ACI committee report recommends that the unit weight can be used as 2.286 gr/cm^3 for normal-density concrete; hence, Eq. (1) reduces to Eq. (2).

$$E = 4700\sqrt{f_c^{'}} \tag{2}$$

Reinforcements are assumed to be linear isotropic material with elastic modulus equal to 210 GPa and Poisson's ratio of 0.3. The mass per unit of steel is taken as 7.850 gr/cm^3 in the initial FE model. Material properties of concrete and reinforcement used in the initial FE models are given in Table 3.

The thickness of the concrete cover was 25 mm. This value is effective in selecting meshing sizes. Since discrete representation is used to model the longitudinal and transverse reinforcements, the concrete and reinforcement nodes must be coincided. To this end, concrete solid element and link element were divided with the same meshing sizes. The concrete volume elements and reinforcement link elements embedded in concrete were divided into 46996 elements with 25x25x25, 25x25x50 and 50x50x50 mm in sizes. Adjacent nodes between solid elements and link elements were connected to each other to represent the perfect bond assumption. Fixed boundary condition was applied to the bottom of the foundation by fixing each direction. Finite element model and its reinforcement layout for the single-story model are shown in Fig. 14.

Numerical modal analysis was carried out for the single-story model to obtain the natural frequencies and mode shapes. The first four natural frequencies calculated were within the 21.497 Hz-43.286 Hz frequencies range. Fig. 15 gives numerically calculated first four mode shapes and natural frequencies. The first two modes are translational modes in the transverse and longitudinal direction, and the third and fourth modes are torsional mode.

Table 3 Material properties for the initial FE model

Element	Material Properties			
	Strength (MPa)	Elasticity Modulus(MPa)	Poisson's Ratio	Density (gr/cm3)
Frame	12	16281	0.20	2286
Foundation	16	18800	0.20	2286
Reinforcement	420	210000	0.30	7.850

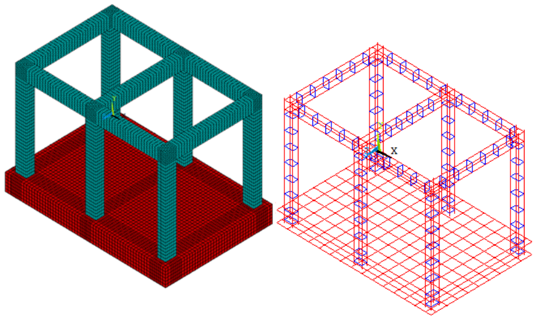

Fig. 14 Finite element model and its reinforcement layout for the single-story model

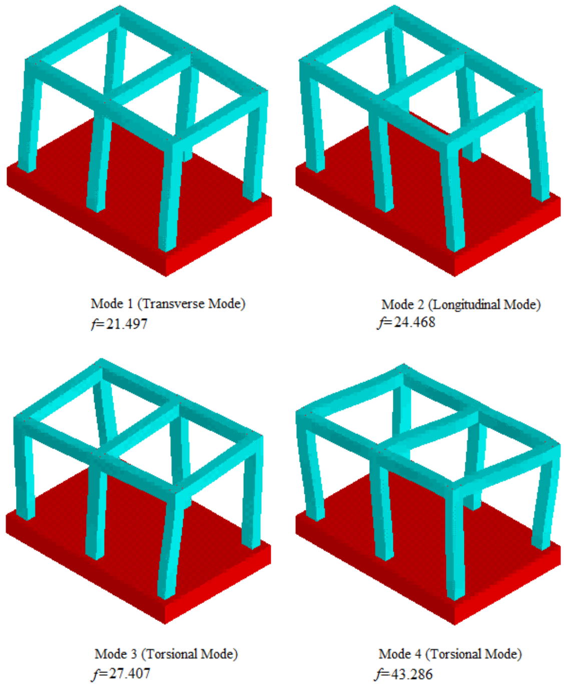

Fig. 15 Numerically calculated mode shapes for the single-story model

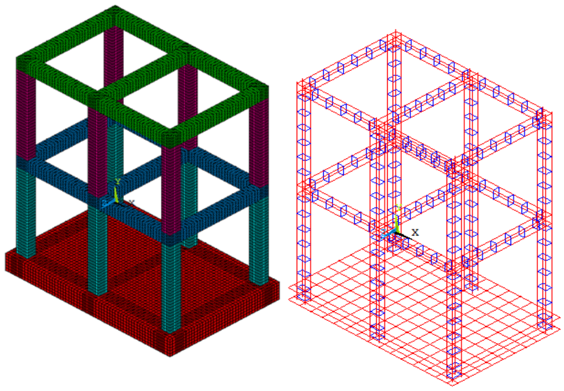

Fig. 16 Finite element model and its reinforcement layout for the two-story model

The two-story model was derived from the single-story model. The initial FE model of the two-story model is shown in Fig. 16. The model includes 69884 elements with 25×25×25, 25×25×50 and 50×50×50 mm in sizes and

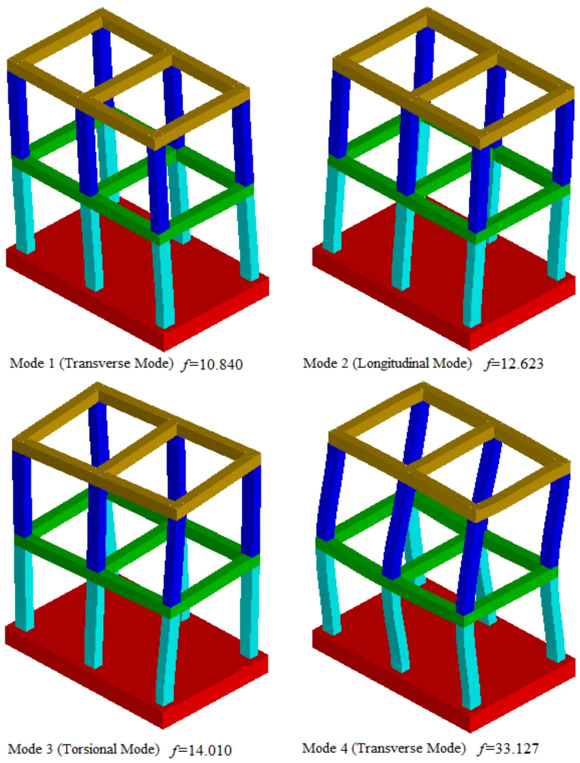

Fig. 17 Numerically calculated mode shapes for the two-story model

Table 4 Numerical and experimental calculated natural frequencies

Mode	Single-Story Model			Two-Story Model		
	Experimental (Hz)	*Diff.* *(%)*	Numerical (Hz)	Experimental (Hz)	*Diff.* *(%)*	Numerical (Hz)
1	25.54	*18.80*	21.497	13.36	*23.25*	10.840
2	28.30	*15.66*	24.468	14.45	*14.47*	12.623
3	34.03	*24.16*	27.407	17.38	*24.05*	14.010
4	55.61	*28.47*	43.286	39.82	*20.20*	33.127

75313 nodes. The same material properties listed in Table 3 were used for the two-story model.

Numerical modal analysis was also carried out for two-story model to obtain the natural frequencies and mode shapes. The first four natural frequencies obtained were within the 10.840 Hz-33.127 Hz frequencies range. Fig. 17 gives the numerically calculated first four mode shapes and natural frequencies. The first two modes are translational modes in the transverse and longitudinal direction, the third mode is torsional mode and the fourth mode is close transverse mode. The FE model and the AVT results show reasonable correlation in terms of mode shapes of the models.

Comparisons of the experimentally and numerically identified natural frequencies for the both models are given in Table 4. As shown in Table 4, there is no clear agreement between the experimental and numerical frequencies. The maximum error between the experimental and numerical frequencies is calculated as 28.47% and 24.05% for the single-story model and two-story model respectively. It can be said that these values are not within the acceptable limits in model updating procedure. Therefore, initial FE models must be updated according to the experimental frequencies.

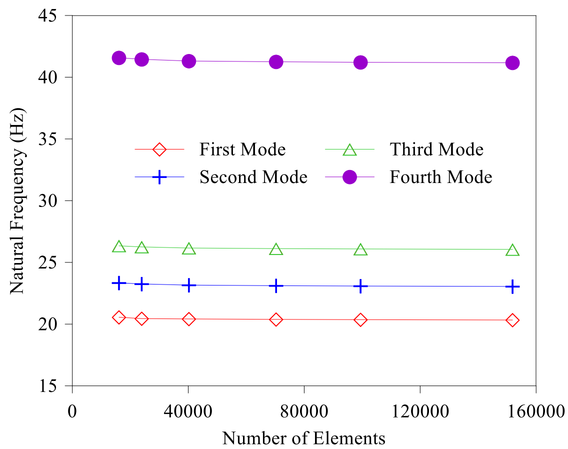

Fig. 18 Convergence study for the suitable meshing sizes

4.2 FE model updating of the single and two-story models

The FE model updating procedure allows us to minimize the errors between the experimental and numerical dynamic characteristics of the structures. In this study, the dynamic characteristics between the experimental and numerical show reasonable correlation in terms of mode shapes. However, some errors are seen between the experimental and numerical calculated frequencies for all modes of single and two-story models. It is thought that these errors may occur due to some uncertainties such as material properties, meshing sizes and boundary conditions. Such errors create a resource of inaccuracy in FE models. Hence, initial FE model of the models must be updated with experimental frequencies.

The choosing of parameters is one of the most important steps in model updating. The number of parameters should be defined to obtain an adequate matching between the experimental and numerical results. Note that for selection of parameters, they should be within the acceptable limits in terms of engineering rules.

Dynamic characteristics depend on the mass and stiffness of structures. Therefore, material properties such as elasticity modulus, mass per unit volume, passion ratio, geometrical properties such as section and additional masses, and modeling properties such as boundary conditions and meshing sizes can be chosen as updating parameters. In the study, because the boundary condition was not very complicate (only bottom side of the raft foundation is fixed to ground), this was not taken into account as an updating parameter. FE models have the same geometry and reinforcement layout with the constructed models; therefore, geometrical parameters were eliminated. The convergence study was performed on the single-story model for the six different meshing sizes to verify the selected meshing size in initial FE models (Fig. 18). It was clearly observed that the suggested meshing sizes were sufficient for the modal analysis.

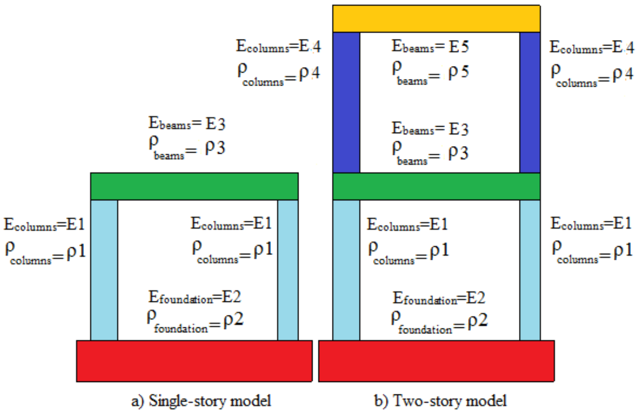

Fig. 19 Material properties variation for each element and story in model updating of single and two story models

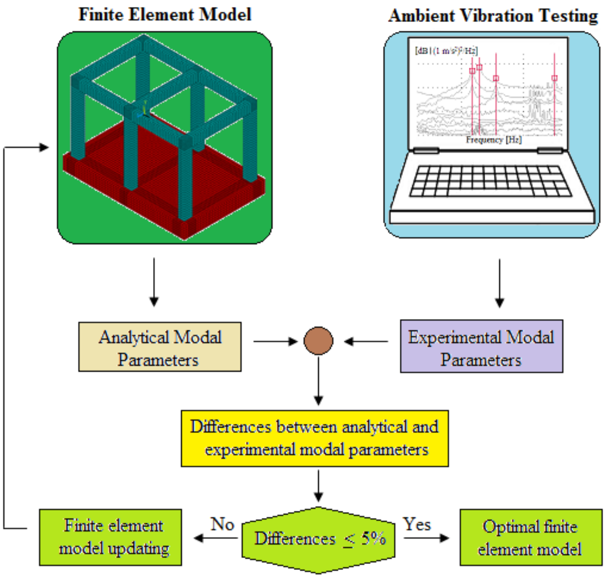

Fig. 20 General flow-chart for the FE model updating

Material properties such as modulus of elasticity and mass per unit volume were selected as updating parameters to minimize the errors between experimental and numerical results. Poisson's ratio is known to have minimal effect on the dynamic response of structures (Atamturktur *et al*. 2012), and therefore a constant values of 0.2 for concrete and 0.3 for steel reinforcement are considered in the analysis. In addition, the elasticity modulus and mass per unit volume of steel reinforcement are also considered as 210000 MPa and 7.850 gr/cm^3, respectively. In the study, the main parameters for the model updating were material properties of concrete such as elasticity modulus and mass per unit volume. These values of concrete were assumed to be not uniform in each element and story. Fig. 19 shows variation of material properties for each element and story.

FE model updating procedure can be practiced using two methods such as manual tuning and automatic model updating using specialized software. In this study, the manual tuning method was used to update the initial FE models. The general flow-chart for the FE model updating procedure is seen in Fig. 20. As seen in Figure, a 5% error between the experimental and analytical results in model updating is an acceptable limit.

In the model updating, selecting the allowable bound of the update parameters were quite difficult and were performed according to the engineering judgment. Elasticity modulus of concrete containing normal strength cement may range from 14000 MPa up to 41000 MPa and its density may ranges between 2240 kg/m^3 and 2400 kg/m^3. Hence, updating parameters can be searched in these ranges.

Manual tuning process was achieved by changing of elasticity modulus and density of concrete. Firstly, the single-story model was updated, and then two-story model was updated with the trial-and-error approach. Table 5 shows the changes in the update parameters before and after model updating for the single and two-story models. After model updating, the maximum changes in elasticity modulus were calculated as 56.02%, 64.00% and 3.72% for columns, beams and foundations, respectively. Also, 0.92% maximum changes were obtained in mass density. The natural frequencies after the model updating are given in Table 6. The maximum errors were reduced from 28.47% to 4.75% and 24.05% to 4.49% for the single-story model and two-story-model, respectively.

Table 5 Changing of material properties for the FE model updating

Updated Parameters	Initial	Updated Values	*Change (%)*
Single-Story Model			
ME of Columns (GPa)	16.28	25.40	*56.02*
ME of Beams (GPa)	16.28	26.70	*64.00*
ME of Foundation(GPa)	18.80	19.50	*3.72*
MD of Columns (kg/m^3)	2286	2297	*0.48*
MD of Beams (kg/m^3)	2286	2307	*0.92*
MD of Foundation (kg/m^3)	2286	2288	*0.09*
Two-Story Model			
ME of Columns (GPa)	16.28	22.50	38.20
ME of Beams (GPa)	16.28	25.20	54.79
MD of Columns (kg/m^3)	2286	2290	0.17
MD of Beams (kg/m^3)	2286	2293	0.30

ME: Modulus Elasticity; ME: Mass Density

Table 6 Comparison of natural frequencies before and after model updating

Mode	Single-Story Model			Two-Story Model		
	Experimental (Hz)	*Diff.* (%)	Numerical (Hz)	Experimental (Hz)	*Diff.* (%)	Numerical (Hz)
1	25.54	*0.97*	25.792	13.36	*2.54*	13.021
2	28.30	*3.33*	29.277	14.45	*4.49*	15.130
3	34.03	*3.29*	32.910	17.38	*3.09*	16.842
4	55.61	*4.75*	52.967	39.82	*1.63*	39.171

5. Earthquake behavior of second-story model

In this section, linear and nonlinear earthquake analysis of two-story model were investigated before and after FE model updating to determine effect of the model updating

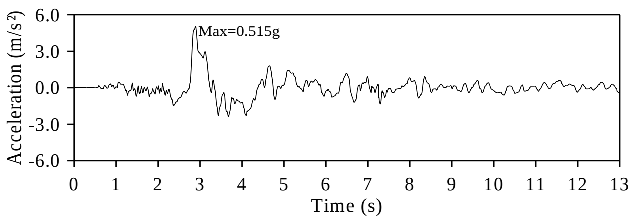

Fig. 21 Time-history of ground motion acceleration of 1992 Erzincan earthquake

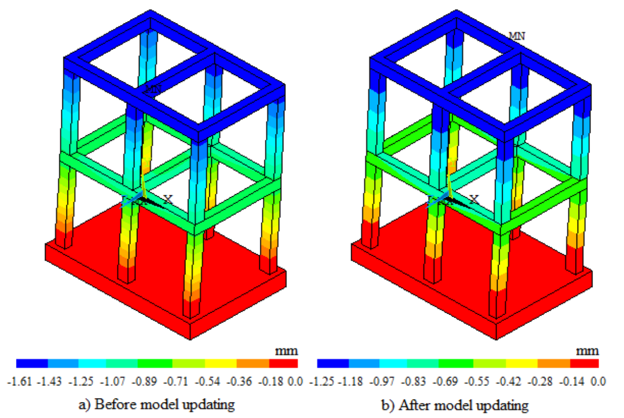

Fig. 22 Maximum displacements contours obtained before and after model updating

procedure on the earthquake behavior. Earthquake analyses were performed using ERZIKAN/ERZ-NS (Fig. 21) component of 1992 Erzincan ground motion (PEER 2012). The peak ground acceleration of NS component was 0.515 g. The motion accelerations were struck to the model in the transverse (*z*) direction where the first mode shape was calculated. A time step of 0.01 second was considered for the earthquake analysis. Gauss numerical integration method was used in the calculation of element matrices. The differential equation of motion was solved by Newmark method. During the dynamic analysis, only first 6.5 second of earthquake motion, which is the most effective duration, was taken into account because of the computational demand of this method and less time consuming. Before model updating, 5% damping ratio was used in the FE analysis. After model updating, 0.985% damping ratio calculated from the AVT was used in the analysis. Rayleigh damping constants calculated considering the first and fourth mode, assuming above values of damping ratios. Alpha and beta coefficients were calculated as 5.1317 and 0.0003620 for the initial condition. These coefficients were calculated as 1.2096 and 0.00006007 for the updated model.

5.1 Linear earthquake analysis results

Linear earthquake analyses were carried out before and after model updating. The time histories of maximum displacements and maximum and minimum principal stresses occurred on nodes were examined as a results of analysis responses. The displacements and stresses contour diagrams were additionally plotted. The time history displacements and stresses were obtained at the 2.85 second

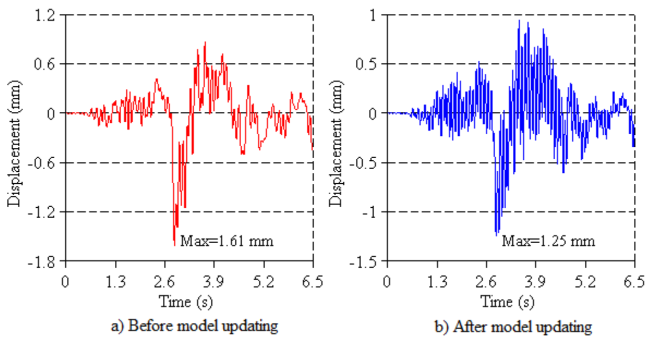

Fig. 23 Time histories of displacements for the initial model (a) and updated model (b)

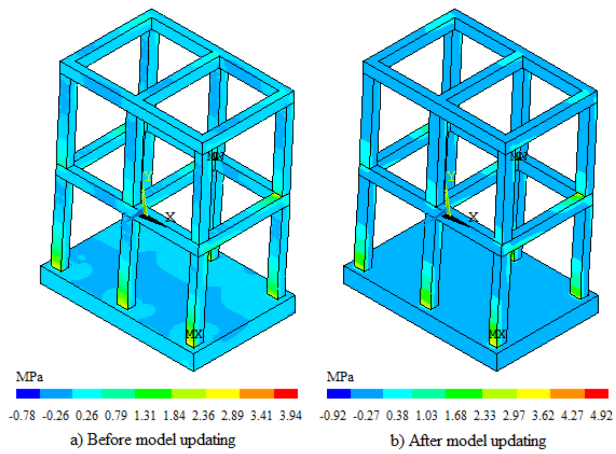

Fig. 24 Maximum principal stress contours before and after model updating

of ground motion (the time when the peak values of maximum displacement and stresses occur on the nodes and elements of the models).

Maximum displacement contours of the models before and after model updating are shown in Fig. 22, respectively. These contours present the distribution of the displacements at the time of 2.85 second. Maximum displacements occurred on the beam-column joints where located central axis of the model.

Time histories of the maximum displacements in the transverse direction (*z*) are plotted in Fig. 23. Maximum displacement at the time of maximum response was calculated as 1.61 mm for the initial model, while the computed displacement for the updated model was 1.25 mm. There was a reduction in displacements after model updating. The maximum difference was calculated as approximately 29%. It should be noted that, the experimental damping ratio was used in the FE analysis of updated model; therefore, results were also affected by the use of experimental damping.

Maximum and minimum principal stress contours of the model obtained for before and after model updating are given in Figs. 24 and 25, respectively. Stress contours show the distribution of the peak values reached by the maximum and minimum stress at each element in the section. Maximum and minimum principal stresses were computed equally (in terms of absolute value) at the column-foundation joints. The frequency content of the stresses

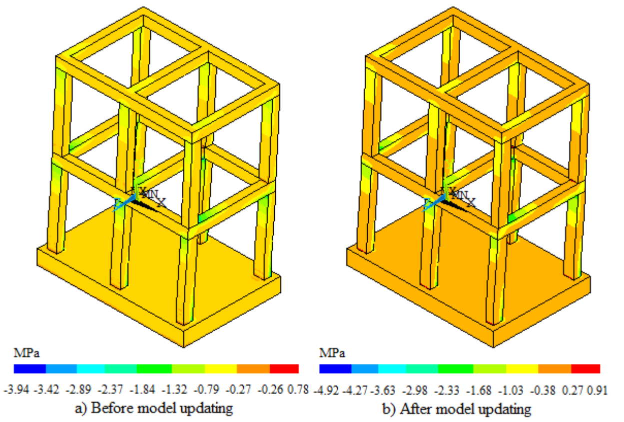

Fig. 25 Minimum principal stress contours before and after model updating

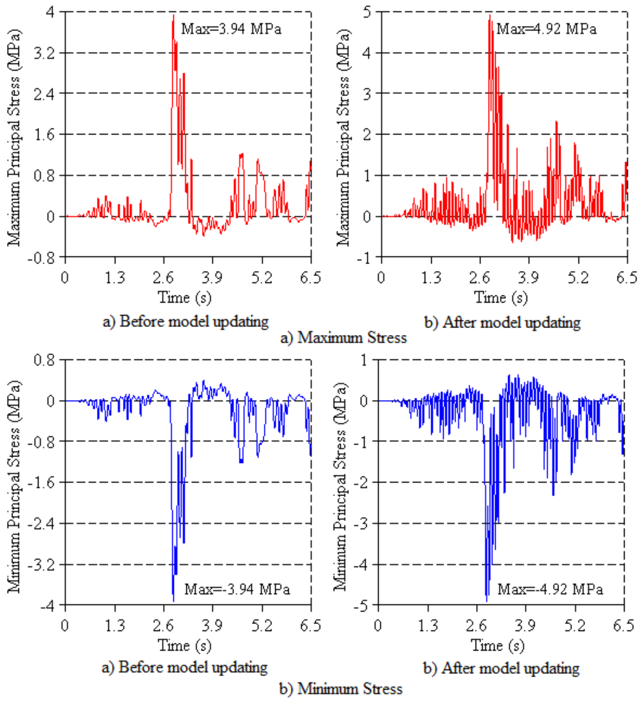

Fig. 26 Time histories of maximum and minimum stresses for the linear analysis

obtained from the updated FE model was different from the initial model.

Time history of the maximum and minimum principal stresses occurred on the nodes for before and after model updating are given in Fig. 26 (a)-(b), respectively. The stresses obtained from the initial model were lower than those of the updated models. Maximum principal stresses were obtained as 3.94 MPa and 4.92 MPa for the initial and updated models, respectively. Minimum principal stresses obtained were -3.94 MPa and -4.92 MPa, respectively, from linear analysis of the initial and updated models of models. After the model updating, maximum differences in the stresses were calculated as 25%.

The results of the linear analysis show that the displacements occurred in the initial model are bigger than those of the updated model, but obtained stresses from the initial model are smaller than those of the updated model. Material properties and damping ratios used in the initial and updated model are different; therefore frequency contents of the displacements and stresses are different. This means that the linear earthquake behaviors of model for the initial and updated models are different.

5.2 Nonlinear earthquake analysis results

In this part, the nonlinear earthquake analyses of second-story model were investigated before and after model updating. The time histories of maximum displacements and maximum and minimum principal stresses with the contour diagrams were examined to investigate the effects of FE model updating on the nonlinear earthquake behavior of the model.

Concrete is a plastic material. ANSYS provides several plasticity approaches to model the compression behavior of concrete. These are: Drucker-Prager (DP) plasticity model, Von-Mises bilinear isotropic hardening model, multi linear isotropic hardening model and multi-linear kinematic hardening model. The DP model proposed by Drucker and Prager (1952) was used for this study to model the nonlinear plastic behavior of concrete. The DP model uses the cohesion and friction angle as material parameters to define yield surface or functions. This model is defined as

$$f = \alpha I_1 + \sqrt{J_2} - k \tag{3}$$

where α and k are constants which depend on cohesion (c) and angle of internal friction (ϕ) of the material given by

$$\alpha = \frac{2\,Sin\phi}{\sqrt{3}\,(3 - Sin\phi)} \qquad k = \frac{6c\ Cos\phi}{\sqrt{3}\ (3 - Sin\phi)} \tag{4}$$

In Eq. (3), I_1 is the first invariant of stress tensor (σ_{ij})

$$I_1 = \sigma_{11} + \sigma_{22} + \sigma_{33} \tag{5}$$

and J_2 is the second invariant of deviatoric stress tensor (s_{ij})

$$J_2 = \frac{1}{2} s_{ij} s_{ij} \tag{6}$$

where s_{ij} is the deviatoric stress as yielded below.

$$s_{ij} = \sigma_{ij} - \delta_{ij}\sigma_m \qquad (i,\ j\ = 1, 2, 3) \tag{7}$$

In Eq. (7), δ_{ij} is the kronecker delta, which is equal to 1 for i=j; 0 for i≠j, and σ_m is the mean stress, expressed as

$$\sigma_m = \frac{I_1}{3} = \frac{\sigma_{11} + \sigma_{22} + \sigma_{33}}{3} = \frac{\sigma_{ii}}{3} \tag{8}$$

If the terms in Eq. (7) are obtained by the Eq. (8) and those are replaced in Eq. (6), the second invariant of the deviatoric stress tensor can be obtained, the expression of which is below.

$$J_2 = \frac{1}{6}\left[(\sigma_{11} - \sigma_{22})^2 + (\sigma_{22} - \sigma_{33})^2 + (\sigma_{33} - \sigma_{11})^2\right] + \sigma_{12}{}^2 + \sigma_{13}{}^2 + \sigma_{23}{}^2 \tag{9}$$

In the study, friction angle (ϕ) was selected to be 32 degrees as recommended by Lubliner *et al*. (1989), Doran *et al.* (1998). The cohesion (c) was calculated using Eq. (10) proposed by Doran *et al.* (1998).

$$c = 0.231 ln(E_0 d^2_{max}) - 0.60 \quad (10)$$

where E_0 is the elasticity modulus of concrete and $d_{\max}$ represents the maximum aggregate sizes in the concrete mix. The cohesion values were calculated for the initial and updated models considering the elasticity modulus of each elements (beam, foundation and column) given in the Table 5. The maximum aggregate size in the concrete mix was 25 mm. For example, the cohesion values for the initial model were calculated as 3.11 MPA and 3.14 MPa for the frame and foundation, respectively.

Bilinear isotropic hardening plasticity (BISO) was used for the material model of reinforcement. The modulus of elasticity and yield strength were 210000 MPa and 420 MPa, respectively. The hardening modulus was assumed to be zero.

ANSYS uses William-Warnke (1975) failure criterion to define the failure surface of concrete. The criterion for failure of concrete due to a multiaxial stress state can be expressed in the form:

$$\frac{F}{f_c} - S \geq 0, \quad (11)$$

F=a function of the principal stress state (σ_{xp}, σ_{yp}, σ_{zp});

S=failure surface expressed in term of principal stresses and five parameters f_t, f_c, f_{cb},

f_1, f_2 given in Table 7;

f_c=Uniaxial crushing stress;

σ_{xp}, σ_{yp}, σ_{zp}=principal stresses in principal directions.

If Eq. (11) is not satisfied, the material will not crack or crush. If all stresses are compressive crushing will occur, however, if any principal stress is tensile the material will crack. A total of five input strength parameters are required to define the failure surface as well as an ambient hydrostatic stress state. They were presented in Table 7.

The failure surface can be identified with a minimum of two parameters, f_t and f_c. The other three constants default to Willam-Warnke (1975) (ANSYS 2015)

$$f_{cb} = 1.2 f_c \quad (12)$$

$$f_1 = 1.45 f_c \quad (13)$$

$$f_2 = 1.725 f_c \quad (14)$$

Table 7 Concrete material table

Label	Description
f_t	Ultimate uniaxial tensile strength
f_c	Ultimate uniaxial compressive strength
f_{cb}	Ultimate biaxial compressive strength
σ_h^a	Ambient hydrostatic stress state
f_1	Ultimate compressive strength for a state of biaxial compression superimposed on hydrostatic stress state σ_h^a
f_2	Ultimate compressive strength for a state of uniaxial compression superimposed on hydrostatic stress state σ_h^a

However, these default values are valid only for stress states where the condition

$$|\sigma_h| \leq \sqrt{3} f_c, \quad (15)$$

$$\sigma_h = \frac{1}{3}(\sigma_{xp} + \sigma_{yp} + \sigma_{zp})$$
$$\sigma_h = hydrostatic\ stresss\ state \quad (16)$$

is satisfied.

Both F function and the failure surface S are expressed in terms of principal stresses denoted as σ_1, σ_2, and σ_3 where

$$\sigma_1 = Max(\sigma_{xp}, \sigma_{yp}, \sigma_{zp}) \quad (17)$$

$$\sigma_3 = Min(\sigma_{xp}, \sigma_{yp}, \sigma_{zp}) \quad (18)$$

and $\sigma_1 \geq \sigma_2 \geq \sigma_3$. The failure of concrete is categorized into four domains:

1. $0 \geq \sigma_1 \geq \sigma_3$ (Compression-compression-compression)
2. $\sigma_1 \geq 0 \geq \sigma_2 \geq \sigma_3$ (Tensile-compression-compression)
3. $\sigma_1 \geq \sigma_2 \geq 0 \geq \sigma_3$ (Tensile-tensile-compression)
4. $\sigma_1 \geq \sigma_2 \geq \sigma_3 \geq 0$ (Tensile-tensile-tensile)

More detailed information related to Willam-Warnke model can be obtained by ANSYS (2015), Help System.

In nonlinear analysis of concrete, shear transfer coefficients (β_t) must be identified. The values of β_t ranges from 0 to 1, with 0 representing a smooth crack and 1 representing a rough crack. In the study, the coefficient for open crack was set to 0.5, while the coefficient for closed crack was set to 1. The uniaxial concrete tensile strength (f_t) were calculated by Eq. (19) (TS 500 2000).

$$f_t = 0.35\sqrt{fc} \quad (19)$$

where: f_c is MPa.

Uniaxial concrete compressive strength (f_c) for the structural elements (beam, column, foundation) of updated model were calculated with Eq. (2) using the elasticity modulus parameters given in Table 5.

The DP plasticity model was combined with the Willam-Warnke failure criterion for the nonlinear analysis of two-story model. Because, it is recommended that combining the failure criterion with a plasticity model will give more accurate results (Kazaz 2010). The ANSYS uses Newton–Raphson equilibrium iterations to update the model stiffness. In the study, for the reinforced concrete solid elements, force and displacement convergence criteria were used as 0.005 and 0.05, respectively.

Maximum displacement contours and the time history of the maximum displacements on the nodes for before and after model updating are given in Fig. 27 (a)-(b), respectively. The time history displacements and stresses were obtained at the 2.90 second of ground motion (the time when the peak values of maximum displacement and stresses occur on the nodes and elements of the models). Maximum nonlinear displacements calculated on the beam-column joints as 3.14 mm and 2.46 mm for the initial model and updated model, respectively. There was a reduction in displacements after model updating. The maximum difference between the initial and updated model was computed as approximately 28%.

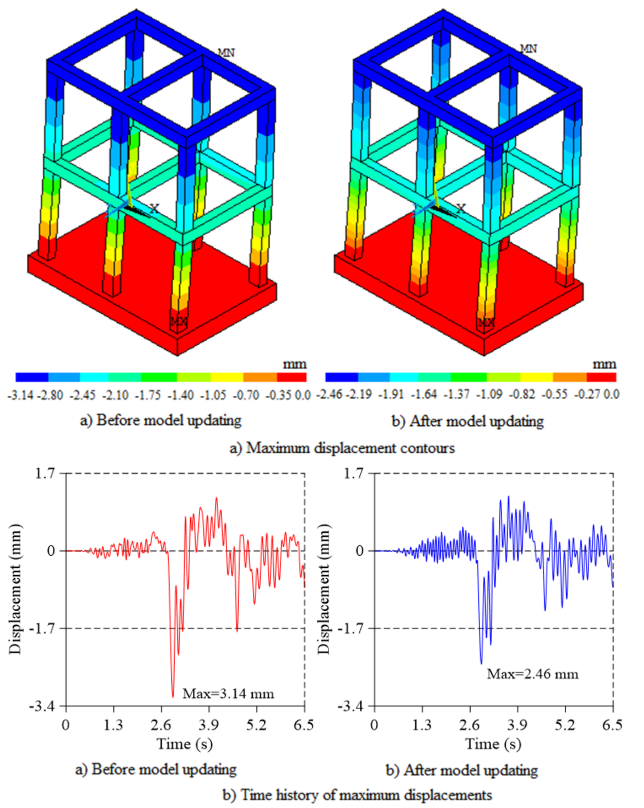

Fig. 27 Maximum displacement contours (a) and the time histories of maximum displacements (b) obtained before and after model updating

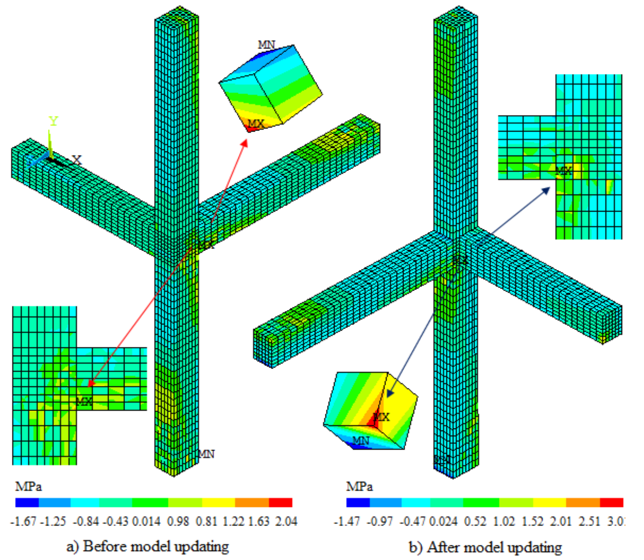

Fig. 28 Maximum principal stress contours for before and after model updating

Maximum and minimum principal stress contours of the model obtained for before and after model updating are shown in Fig. 28 and 29, respectively. Stress contours indicate the distribution of the peak values reached by the maximum and minimum stress at each element in the section. Maximum principal stresses were occurred in different place of the beam-column joints located over the first story. Minimum principal stresses were obtained in the different part of the column-foundation joints. As seen in Fig. 28 and 29, the frequency content of the stresses obtained from the updated FE model was different from the initial model.

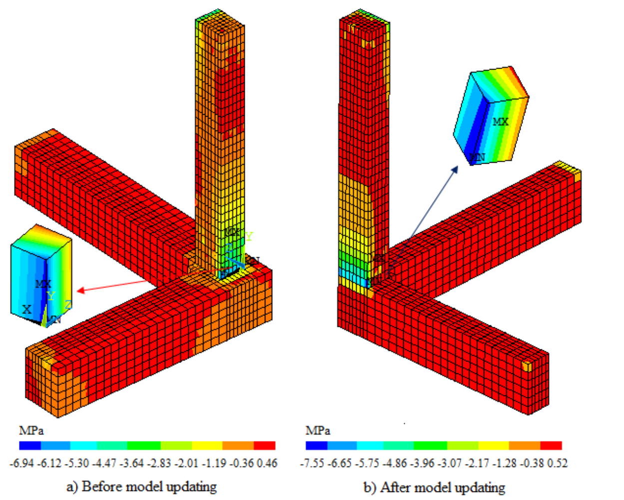

Fig. 29 Minimum principal stress contours for before and after model updating

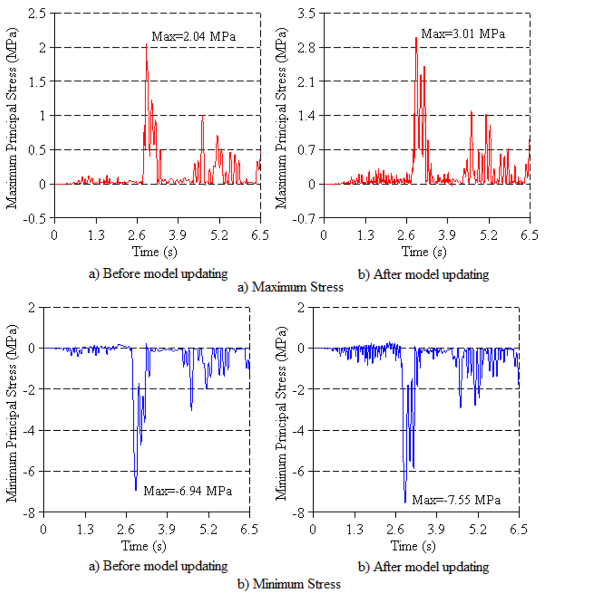

Fig. 30 Time histories of maximum and minimum stresses for the nonlinear analysis

Time history of the maximum and minimum principal stresses occurred on the nodes for before and after model updating are plotted in Fig. 30 (a)-(b), respectively. Stresses obtained updated model was bigger than those of the initial model. The maximum principal stresses were obtained as 2.04 MPa and 3.01 MPa for the initial and updated models, respectively. Minimum principal stresses obtained were -6.94 MPa and -7.55 MPa for the initial and updated model, respectively. After the model updating, the maximum differences in the stresses were calculated as 47%. Similar to the linear analysis, the displacements occurred in the initial model are bigger than those of the updated model, and the obtained stresses from the initial model are smaller than those of the updated model. The results indicate that

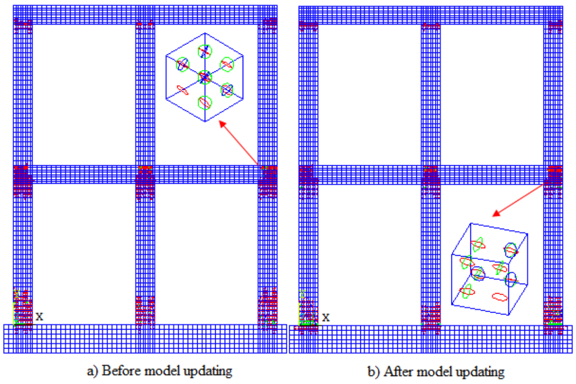

Fig. 31 Crack distribution obtained from the initial (a) and updated (b) models

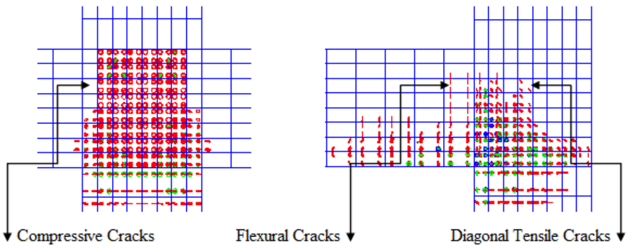

Fig. 32 Typical cracking signs observed in finite element models

the FE model updating have a significant effect on the earthquake behavior of models.

Cracking distributions for the initial and updated models were obtained with the Crack/Crushing command in ANSYS. In software, cracking and crushing sings are shown with a circle and an octahedron in the plane of the crack. If the crack has opened and then closed, the circle outline will have an *X* through it. First crack at an integration points is represented with a red circle outline, the second crack with a green outline, and third crack with a blue outline (ANSYS 2015). Only cracking sings were observed in the models. First cracks for the initial and updated models were obtained at the 2.81 second and 2.40 second of ground motion, respectively. First cracks occurred around the column-foundation joints and beam-column joints when the principal tensile stress exceed the ultimate tensile strength of concrete which were at 1.21 MPa and 1.54 MPa for the initial and updated models, respectively. Fig. 31 shows the plots of the crack distributions for the initial and updated models. Crack distributions were plotted at the 2.90 second of ground motion where the maximum stresses were obtained. As seen Fig. 31, most cracks concentrated in the region of column-foundation joints and beam-column joints. The similar crack distributions were observed in general for both the initial and updated models. Three typical cracking signs were observed in the models. The cracking signs observed in models are given in Fig. 32.

5.3 Comparison of linear and nonlinear earthquake analysis results

Linear and nonlinear earthquake analysis of two-story model was performed for the initial and updated models. Here, the earthquake analysis results for both methods were compared with each other. Table 8 compares maximum displacements, maximum and minimum principal stresses obtained from the linear and nonlinear earthquake results. As expected, the trend was for the displacements to increase significantly with the nonlinear analysis. The maximum differences were calculated as 95% and 97% for the initial and updated models, respectively. Maximum principal stresses obtained from the linear analysis were greater than the stresses of the nonlinear analysis. Maximum differences were 93% and 64% for the initial and updated models. In addition, minimum principal stresses increase with the nonlinear analysis compared to linear analysis. The calculated maximum differences in minimum principal stresses were 76% and 54% for the initial and updated models.

Table 8 Comparison of linear and nonlinear obtained results for the initial and updated model

Parameters	Initial Model			Updated Model		
	Linear	*Diff.(%)*	Nonlinear	Linear	*Diff.(%)*	Nonlinear
MD (mm)	1.61	95	3.14	1.25	97	2.46
MPS1	3.94	93	2.04	4.92	64	3.01
MPS2	-3.94	76	-6.94	-4.92	54	-7.55

MD: Maximum Displacement; MPS1: Maximum Principal Stress
MPS2: Minimum Principal Stress

6. Conclusions

The objective of this study was to investigate the effects of the model updating on the linear and nonlinear earthquake behavior. A 1/2 geometrically scale, two-storey, reinforced concrete frame model was considered as sample for examining the obtained results. Ambient vibration test was used to identify the dynamic characteristics experimentally. ANSYS software used to obtain the dynamic characteristics of model numerically. The linear and nonlinear earthquake analyses were carried out using 1992 Erzincan earthquake record to determine the effects of the finite element model updating. From the study, the following conclusions can be drawn:

Experimental Measurements

- Natural frequencies obtained from the EFDD and SSI methods were close to each other.
- Natural frequencies were obtained within the 0-100Hz and 0-50 Hz ranges for the single-story and two-story model, respectively.
- First four mode shapes obtained from the experimental measurements of two-story model. The first one was transverse mode, the second one was longitudinal mode, the third one was torsional mode and fourth was transverse mode.
- First four frequencies were identified within 25.54 Hz-55.61 Hz and 13.36 Hz-13.36 Hz-39.82 Hz (for the EFDD) for the single-story model and two-story model,

respectively.

Initial FE model

• First four natural frequencies were calculated in the range of 21.497 Hz-43.286 Hz from the initial FE model of single-story model.

• First four natural frequencies obtained were within the 10.840 Hz-33.127 Hz frequencies range for the two-story model.

• Maximum errors between the experimental and numerical frequencies were calculated as 28.47% and 24.05% for the single-story model and two-story model respectively.

FE model updating

• Manuel tuning procedure was used for the FE model updating.

• Modulus of elasticity and mass per unit volume were selected as updating parameters. These values were assumed to be not uniform in each element and story.

• A 5% error between the experimental and analytical results in model updating was chosen as an acceptable limit.

• With the model updating, the maximum errors were reduced from 28.47% to 4.75% and 24.05% to 4.49% for the single-story model and two-story-model, respectively.

• There was a clear agreement between the mode shapes before and after model updating.

• Damping ratio with the value of 5% and 0.985% were used for the initial model and updated model.

Linear analysis results

• Maximum displacement at the time of maximum response (2.85 second) was calculated as 1.61 mm and 1.25 mm for the initial model and updated model. Maximum displacements occurred on the beam-column joints of the second story.

• Maximum and minimum principal stresses computed equally (in terms of absolute value) at the column-foundation joints. The maximum principal stresses were calculated as 3.94 MPa and 4.92 MPa for the initial and updated models.

• After the model updating, maximum differences in the displacements and stresses were calculated as 29% and 25%.

Nonlinear analysis results

• Maximum nonlinear displacements at the time of maximum response (2.90 second) calculated on the beam-column joints as 3.14 mm and 2.46 mm for the initial model and updated model.

• Maximum and minimum principal stresses were occurred in different place of the beam-column joints and the column-foundation joints for the initial and updated models.

• Maximum and minimum principal stresses were obtained as 2.04 MPa and -6.94 MPa for the initial model. After model updating, the maximum and minimum principal stresses obtained were 3.01 MPa and -7.55 MPa.

• After model updating, maximum differences in the displacements and stresses were computed as 28% and 47%.

• First cracks for the initial and updated models were obtained at the 2.81 second and 2.40 second of ground motion, respectively. Most of the cracks concentrated at the column-foundation joints and beam-column joints. Compressive, flexural and diagonal tensile cracks were observed in the initial and updated model. The similar crack distributions were almost observed for both models.

• Maximum differences between the linear and nonlinear analysis for the displacements and stresses were calculated as 97% and 93%. The nonlinear earthquake results were considerably difference from the linear analysis. Therefore, the simulation of the structural behavior under dynamic loading requires nonlinear analysis to have meaning results.

The conclusion of the study strongly suggests that the finite element model updating procedure must be carried out to obtain the accurate FE model of structures. Because, the obtained results, especially nonlinear analysis results changed very significantly after model updating.

Acknowledgments

This research has been supported by the Karadeniz Technical University under Research Grant No: 8940.

References

ACI Committee 318 (2008), Building Code Requirements for Structural Concrete (ACI 318M-11) and Commentary, American Concrete Institute, Farmington Hills, MI, USA.

Alampalli, S. (2000), “Effects of testing, analysis, damage, and environment on modal parameters”, *Mech. Syst. Signal Pr.*, **14**(1), 63-74.

Altunışık, A.C., Bayraktar, A., Sevim, B. and Özdemir, H. (2011), “Experimental and analytical system identification of Eynel Arch Type Steel Highway Bridge”, *J. Constr. Steel Res.*, **67**(12), 1912-1921.

Altunışık, A.C., Günaydın, M., Sevim, B., Bayraktar, A., and Adanur, S. (2015), “CFRP composite retrofitting effect on the dynamic characteristics of arch dams”, *Soil Dyn. Earthq. Eng.*, **74**, 1-9.

ANSYS (2015), Swanson Analysis System, US.

ANSYS® APDL, Release 14.5 (2015), Help System, Coupled Field Analysis Guide, ANSYS, Inc.

Atamturktur, S., Hemez, F.M. and Laman, J.A. (2012), “Uncertainty quantification in model verification and validation as applied to large scale historic masonry monuments”, *Eng. Struct.*, **43**, 221-234.

Bendat, J.S. and Piersol, A.G. (2004), *Random Data: Analysis and Measurement Procedures*, John Wiley and Sons, USA.

Bonfiglioli, B. and Pascale, G. (2006), “Dynamic assessment of reinforced concrete beams repaired with externally bonded frp sheets”, *Mech. Compos. Mater.*, **42**(1), 1-12.

Brownjohn, J.M.W. (1997), “Vibration characteristics of a suspension footbridge’’, *J. Sound Vib.*, **202**, 29-46.

Brownjohn, J.M.W., Dumanoğlu, A.A. and Severn, R.T. (1992), "Ambient vibration survey of the Fatih Sultan Mehmet (Second Bosporus) suspension bridge", *Earthq. Eng. Struct. Dyn.*, **21**, 907-924.

Cantero, D., Hester, D., and Brownjohn, J. (2017), "Evolution of bridge frequencies and modes of vibration during truck passage", *Eng. Struct.*, **152**, 452-464.

Chang, C.C., Chang, T.Y.P. and Zhang, Q.W. (2001), "Ambient vibration of long-span cable-stayed bridge", *ASCE J. Bridge Eng.*, **1**, 46-53.

Chen, G.W., Omenzetter, P. and Beskhroun, S. (2017), "Operational modal analysis of an eleven-span concrete bridge subjected to weak ambient excitations", *Eng. Struct.*, **151**, 839-860.

Deinum, P.J., Dungar, R., Ellis, B.R., Jeary, A.P., Reed, G.A.L. and Severn, R.T. (1982), "Vibration tests on Emosson arch dam in Switzerland", *Earthq. Eng. Struct. Dyn*., **10**(3), 447-70.

Diaferio, M., Foti, D. and Potenza, F. (2018), "Prediction of the fundamental frequencies and modal shapes of historic masonry towers by empirical equations based on experimental data", *Eng. Struct.*, **156**, 433-442.

Doebling, S.W., Farrar, C.R., Prime, M.B. and Shevitz, D.W. (1996), "Damage identification and health monitoring of structural and mechanical systems from changes in their vibration characteristics: A literature review", Research Rep. No. LA-13070-MS, ESA-EA, Los Alamos National Laboratory, Los Alamos, N.M.

Doran, B., Köksal, H.A., Polat, Z. and Karakoç, C. (1998), "The use of "Drucker-Prager Criterion" in the analysis of reinforced concrete members by finite elements", *Turkish Chamb. Civil Eng.*, **9**(2), 1616-1625.

Drucker, D.C. and Prager, W. (1952), "Soil mechanics and plastic analysis or limit design", *Quart. Appl. Math.*, **10**, 157-165.

Ewins, D.J. (1984), *Modal Testing: Theory and Practice*, Research Studies Press Ltd, Baldock, Hertfordshire, England.

Felber, A.J. (1993), "Development of hybrid bridge evaluation system", PhD Thesis, University of British Columbia, Vancouver, Canada.

Friswell, M.I. and Mottershead, J.E. (1995), *Finite Element Model Updating in Structural Dynamics*, Kluwer Academic, Dordrecht, The Netherlands.

Hassiotis, S. and Jeong, G.D. (1995), "Identification of stiffness reductions using natural frequencies", *J. Eng. Mech*., ASCE, **121**, 1106-1113.

Jacobsen, N.J., Andersen, P. and Brincker, R. (2006), "Using enhanced frequency domain decomposition as a robust technique to harmonic excitation in Operational Modal Analysis", *Proceedings of ISMA2006: International Conference on Noise & Vibration Engineering*, Leuven, Belgium.

Jaishi, B. and Ren, W.X. (2005), "Structural finite element model updating using ambient vibration test results", *J. Struct. Eng.*, **131**(4), 617-628.

Jaishi, B., Kim, H.J., Kim, M.K., Ren, W.X. and Lee, S.H. (2007), "Finite element model updating of concrete-filled steel tubular arch bridge under operational condition using modal flexibility", *Mech. Syst. Signal Pr.*, **21**, 2406-2426.

Kaiser, H. and Karbhari, V.M. (2004), "Non-destructive testing techniques for FRP rehabilitated concrete. I. A critical review", *Int. J. Mater. Prod. Technol.*, **21**(5), 349-384.

Kazaz, İ. (2010), "Dynamıc characteristics and performance assessment of reinforced concrete structural walls", PhD Thesis, Middle East Technical University, Turkey.

Kouris, L.A.S., Penna, A. and Magenes, G. (2017), "Seismic damage diagnosis of a masonry building using short-term damping measurements", *J. Sound Vib*., **394** 366-391.

Loh, C.H. and Wu, T.S. (1996), "Identification of Fei-Tsui arch dam from both ambient and seismic response data", *Soil Dyn. Earthq. Eng.*, **15**, 465-483.

Lubliner, J., Oliver, J., Ollers, S. and Onate, E. (1989), "A plastic-damage model for concrete", *Int. J. Solid Struct.*, **25**(3), 299-326.

Oliveira, S. and Mendes P. (2006), "Development of a Cibril Dam finite element model for dynamic analysis using ambient vibration tests results", *Proceedings of the III European Conference on Computational Mechanics Solids, Structures and Coupled Problems in Engineering*, Lisbon, Portugal, June.

OMA (2006), Operational Modal Analysis, Release 4.0, Structural Vibration Solutions A/S, Denmark.

Park, H.S. and Oh, B.K. (2018), "Damage detection of building structures under ambient excitation through the analysis of the relationship between the modal participation ratio and story stiffness", *J. Sound Vib.*, **418**, 122-143.

PEER (2012), Pacific Earthquake Engineering Research Centre, http://peer. berkeley.edu/smcat/data, 11.06.2012.

Peeters, B. (2000), "System identification and damage detection in civil engineering", PhD Thesis, K.U, Leuven, Belgium.

Proulx, J., Paultre, P., Rheault, J. and Robert, Y. (2001), "An experimental investigation of water level effects on the dynamic behavior of a large arch dam", *Earthq. Eng. Struct. Dyn.*, **30**(8), 1147-1166.

PULSE (2006), Analyzers and Solutions, Release 11.2, Bruel and Kjaer, Sound and Vibration Measurement A/S, Denmark.

Rainieri, C., Fabbrocino, G., Cosenza, E. and Manfredi, G. (2007), "Implementation of OMA procedures using labview: theory and application", *2nd International Operational Modal Analysis Conference*, Copenhagen, Denmark, April-May.

Ren, W.X. and De Roeck, G. (2002a), "Structural damage identification using modal data. I: Simulation verification", *J. Struct. Eng*., **128**(1), 87-95.

Ren, W.X. and De Roeck, G. (2002b), "Structural damage identification using modal data. II: Test verification", *J. Struct. Eng*., **128**(1), 96-104.

Ren, W.X., Zhao, T. and Harik, I.E. (2004), "Experimental and analytical modal analysis of steel arch bridge", *J. Struct. Eng.*, ASCE, **130**(7), 1022-1031.

Ribeiro, D., Calçada, R., Delgado, R., Brehm, M. and Zabel, V. (2012), "Finite element model updating of a bowstring-arch railway bridge based on experimental modal parameters", *Eng. Struct.*, **40**, 413-435.

Sevim, B., Bayraktar, A. and Altunışık, A.C. (2011), "Finite element model calibration of Berke arch dam using operational modal testing", *J. Vib. Control*, **17**(7), 1065-1079.

Skolnik, D., Yu, E., Wallace, J. and Taciroglu, E. (2007), "Modal system identification and finite element model updating of a 15-story building using earthquake and ambient vibration data", *SEI2007, Structural Engineering Institute*, California, USA, May.

Sortis, A.D., Antonacci, E. and Vestroni, F. (2005), "Dynamic identification of a masonry building using forced vibration tests", *Eng. Struct.*, **27**, 155-165.

TS 500 (2000), Turkish Standart, Requirements for Design and Construction of Reinforced Concrete Structures, Turkey.

Türker, T. and Bayraktar, A. (2014), "Evaluation of damage effects on dynamic characteristics of RC buildings by ambient vibration test", *J. Test. Eval.*, **42**(2), 398-411.

Ventura, C.E., Lord, J.F. and Simpson, R.D. (2002), "Effective use of ambient vibration measurements for model updating of a 48 storey building in Vancouver, Canada", *International Conference on Structural Dynamics Modelling-Test, Analysis, Correlation and Validation*, Instituto de Engenharia Mecanica, Madeira Island, Portugal.

Wang, B.S. and He, Z.C. (2007), "Crack detection of arch dam using statistical neural network based on the reductions of natural frequencies", *J. Sound Vib*., **302**, 1037-1047.

Willam, K.J. and Warnke, E.D. (1975), "Constitutive model for the triaxial behavior of concrete", *Intl. Assoc. Bridge Struct. Eng.*, **19**, 174-203.

Wu, J.R. and Li, Q.S. (2004), "Finite element model updating for a high-rise structure based on ambient vibration measurements", *Eng. Struct.*, **26**, 979-990.

Yang, J., Jin, F., Wang, J.T. and Kou, L.H. (2017), "System identification and modal analysis of an arch dam based on earthquake response records", *Soil Dyn. Earthq. Eng.*, **92**, 109-121.

Zhou, X.T., Ko, J.M. and Ni, Y.Q. (2007), "Experimental study on identification of stiffness change in a concrete frame experiencing damage and retrofit", *Struct. Eng. Mech.*, **25**(1), 39-52.

Ziyad, D. (1988), "Experimental and finite element studies of a large arch dams", Ph.D. Thesis, California Institute of Technology, USA.

Zonta, D., Elgamal, A., Fraser, M. and Nigel Priestley, M.J. (2008), "Analysis of change in dynamic properties of a frame-resistant test building", *Eng. Struct.*, **30**, 183-196.

CC